Study of Prediction Methods for NOx Emission from Turbofan Engines

N. Chandrasekaran* and Abhijit Guha†

Indian Institute of Technology Kharagpur, Pin 721 302, India

DOI: 10.2514/1.B34245

Protecting the environment from the consequences of human activity has become a major challenge and goal in recent years, and therefore such considerations have become a critical component of engineering design and operation as well as of the formulation of policies and legislation. Emission from aircraft engines is a major environmental issue. To assess and control aircraft emission, one needs an accurate tool for predicting it reliably. Many methods of prediction are available for NOx emission index in the open literature, while some methods used by the industries require proprietary information. This paper brings together many important prediction methods (listed in the Appendix) and makes a systematic study of their accuracy and applicability. Finally, a new method called *NOx: generic* is proposed here, which compares well with the most dependable method (preferred by the industries), viz., the $P_3 - T_3$ method, but unlike the $P_3 - T_3$ method the present formulation does not require any proprietary information.

Nomenclature

D_p	=	mass of NOx emitted during the landing and takeoff cycle, g
F	=	air fraction in primary zone
F_{oo}	=	rated output of the engine, kN
H	=	humidity factor
h	=	specific humidity, kg of water per kg of dry air
Ma	=	Mach number
P_{amb}	=	ambient pressure, kPa
P_3	=	combustor inlet pressure, kPa
p_3	=	combustor inlet pressure, psia
T_{amb}	=	ambient temperature, K
T_{fl}	=	flame temperature, K
T_{pz}	=	temperature in the primary zone of the combustor, K
T_λ	=	flame temperature for stoichiometric combustion, K
T_3	=	combustor inlet temperature, K
T_4	=	combustor outlet temperature, K
t_{form}	=	formation time of NOx in the combustion chamber, s
t_{res}	=	residence time in the combustion chamber, s
t_3	=	combustor inlet temperature, °R
V_c	=	combustor volume, m³
V_{jc}	=	fully expanded jet speed of the cold bypass stream, m/s
V_{jh}	=	fully expanded jet speed of the hot core stream, m/s
W_a	=	combustor inlet airflow rate, kg/s
W_f	=	fuel flow rate, kg/s
ΔP_3	=	liner pressure drop in the combustion chamber, kPa
δ_{amb}	=	ratio of flight level ambient pressure to sea level ambient pressure
δ_i	=	ratio of flight level pressure at engine intake to sea level ambient pressure
η_f	=	isentropic efficiency of the fan
η_{LPT}	=	isentropic efficiency of the low-pressure turbine
θ_{amb}	=	ratio of flight level ambient temperature to sea level ambient temperature
θ_i	=	ratio of flight level temperature at engine intake to sea level ambient temperature

Subscripts

FL	=	flight level condition
SL	=	sea level condition
TO	=	takeoff

I. Introduction

THIS paper provides a systematic study of the prediction methods for NOx emission from aircraft gas turbine engines and proposes a modified method based on nonproprietary data. Currently, the total amount of emission of NOx and other species from worldwide fleet of aircraft is less than that of land-based vehicles. However, emissions from aircraft have become a very important issue because cruise emissions in the upper troposphere [1,2] and lower stratosphere [2] directly contribute to the climate change. The worldwide fleet of aircraft is expected to grow by more than a factor of two in the next two decades [3] which may worsen the situation further. Any possible reduction in the emission due to improvement in technology will not be able to counteract the increase in emission due to the growth in aviation [4]. To restrict the effect on global warming, the regulations or legislations for engines and aircraft are expected to be made more stringent. From the brief discussion on regulations given in the next section, it becomes clear that the major emphasis of regulatory control is on the NOx emission. Therefore, the accurate prediction and assessment of NOx emission from engines during all phases of an aircraft mission become essential.

Aircraft emissions include carbon dioxide (CO_2), water vapor (H_2O), sulfur oxide (SO_x), nitrogen dioxide (NO_2), nitrous oxide (N_2O), carbon monoxide (CO), unburned hydrocarbons (UHC), soot, and particulate matter. Typical cruise emissions of a modern turbofan engine consist of 72% CO_2, 27.5% H_2O, 0.02% SO_x, and 0.4% trace species. The trace species in turn contains 84% NOx, 11.8% CO, 4% UHC, and 0.2% soot [4].

Among the emissions listed previously, main contributors for climate change are CO_2 (a direct greenhouse gas [4]), soot, H_2O, and NOx (indirect greenhouse gases [4]). Soot and H_2O emission lead to contrail and cirrus cloud formation, whereas NOx leads to a change in methane and ozone [4]. Ozone enhances the greenhouse effect at the low temperature of cruise altitude more than at sea level (SL). CO_2 and H_2O emissions can be directly estimated from the fuel burn,

whereas NOx emission cannot be estimated directly because it depends also on the way the combustion is controlled.

Therefore, the prediction of NOx emission is complex and has become an active research area. As a result, various prediction methods are available in the open literature, although some methods used by the industries require proprietary information. This paper brings together many such important prediction methods (listed in the Appendix) and makes a systematic study about their accuracy and applicability. Finally, a new method is proposed here, which compares well with the most dependable method (preferred by the industries), viz., the $P_3 - T_3$ method, but unlike the $P_3 - T_3$ method the present formulation does not require any proprietary information.

II. Engine Testing, Databank, and Regulations

The International Civil Aviation Organization (ICAO), United Nations, frames rules, guidelines, and certification of air navigation for existing and future engines and ensures safe and orderly growth of air transport. The emission standards formulated by the ICAO in "Annex 16: environmental protection, volume 2: aircraft engine emissions to the convention on international civil aviation" [5] are the regulations that are to be followed by all the aircraft engine manufacturers. In this document, upper limits for all major pollutant emissions (CO, HC, NOx, and soot emissions) during standardized landing and takeoff (LTO) cycle are specified for all existing and future turbojet and turbofan engines.

The term *smoke number* is used to define soot emissions, and its regulation came into effect in 1983. The limits for other gaseous emissions like NOx, CO, and UHC started from the year 1986, and they were applicable to those engines whose takeoff thrust exceeded 26.7 kN at international standard atmosphere SL static (SLS) condition. The existing regulation of the ICAO for NOx, CO, UHC, and smoke are for LTO. An LTO cycle includes four phases of an aircraft mission based on throttle settings: takeoff (100% thrust), climbout (85% thrust), approach (30% thrust) and idle (7% thrust), and it covers only up to 3000 ft altitude. The engine manufacturers have to test their engines for various throttle settings at SLS condition, and values from such tests are to be listed in the ICAO databank [6], which is publicly available. The characteristic level of gaseous pollutants D_p/F_{oo} (in g/kN) is the basis for certifying engines, where D_p is the mass of NOx emitted during the LTO cycle, and F_{oo} is the rated output (RO) of the engine. It is a function of the time in mode (TIM), emission index (EI), fuel flow rate (W_f), and RO engine thrust specified in the ICAO aircraft engine emissions databank:

$$\frac{D_p}{F_{oo}} = \sum_i \text{EI}_i \cdot \text{TIM}_i \cdot \frac{W_f}{\text{RO}} \tag{1}$$

in which the summation is over the ICAO LTO cycle and the index *i* represents the four throttle settings. EI is defined as the ratio of grams of a particular pollutant to kilograms of fuel burned (in g/kg). Unlike D_p/F_{oo}, EI is used for entire mission including cruise to calculate the amount of emission from the aircraft.

Over the past four decades, the specific fuel consumption (SFC), noise, and UHC emission are all reduced (by 70, 50, and 90%, respectively), but the NOx emissions for commercial aircraft in the same time period have increased by approximately 10% [7]. This is so because the research on aircraft engines has focused mainly on improving engine fuel efficiency, which often leads to an increase in NOx emissions. The increase in thermal efficiency was achieved by

the use of improved blade cooling methods and temperature-resistant materials, thereby enabling the use of higher maximum temperature in the cycle and higher overall pressure ratio (OPR). The OPR has approximately increased from 20 to 40, and the turbine entry temperature (TET) has correspondingly increased by 350°C, resulting in an increase of thermal efficiency from 48 to 55% [8].

Table 1 lists overall characteristics of the various types of combustor generations. Currently, the dominant type existing in the market is the generation-three combustor. A higher generation indicates a higher level of technology and thus a reduction in NOx emission at a given OPR and TET. But the use of higher OPR (and correspondingly higher TET), as explained in the previous paragraph, would tend to offset the reduction of NOx emission achieved through improved combustor design.

The regulation level set by the ICAO in 1993 for NOx had a linear relation with OPR. The regulation has been revised three times already (ICAO 1993, ICAO 1999, and ICAO 2005), due to its high influence on climate change. Hence, the allowed level of NOx emission depends on the date of manufacture of the engine. According to the latest regulation, the allowed limit of NOx emission is a function of OPR and maximum takeoff thrust. The emission standards proposed by the Committee on Aviation Environmental Protection (CAEP, a technical committee formed by the ICAO to assist the council in making new policy and standards for aircraft emissions and noise level) are becoming more stringent, and they may cover cruise emissions in the near future. Figure 1 shows the various NOx emission standards available at present (data taken from [5,9]). The most recent standard incorporated into Annex 16 is CAEP/8, in which a 15% more stringent NOx standard is proposed on the current standard, and its effective date is 31 December 2013. The effective date for the production cutoff of engines according to the current standard is 31 December 2012. The CAEP/8 goals [5] are 1) a medium-term goal (2016) of CAEP/6 levels −45%, ±2.5% (of CAEP/6) at an OPR of 30 and 2) a long-term goal (2026) of CAEP/6 levels −60%, ±5% (of CAEP/6) at an OPR of 30.

Despite the upper limits for pollutant emissions from aircraft (set by the ICAO regulations), policy makers in some countries are announcing incentives for the airlines based on the emissions [10]. Such market-based approaches encourage the airlines to use best-in-class engine technology. These include emission dependent landing fees, emission dependent en route charges, and emissions trading of airline CO_2 and other gases.

Among the approaches stated, the first is already in practice at a few airports, whereas the rest are being discussed in Europe [10]. Presently, the landing fee is charged on the basis of LTO cycle NOx emissions. In the emission-dependent landing fees approach, OPR is not taken into consideration, which is different from the ICAO standards. Emission factors are calculated for each aircraft, and the grouping of aircrafts is done into different emission classes. Landing fee rebates are offered to the aircrafts depending upon the emission class. A standard for this approach of NOx-dependent landing fee was adopted as a European Civil Aviation Conference recommendation in 2003 [11].

Advisory Council for Aeronautics Research in Europe (ACARE) 2020 goals [12] are proposed in Europe that set individual targets for

Table 1 Variation in NOx emission with the combustor generation

Combustor generation	OPR range	Characteristic NOx range, g/kN
1	18–20	70–80
2	27–34	90–110
3	19–42	30–92
4	22–31	30–41

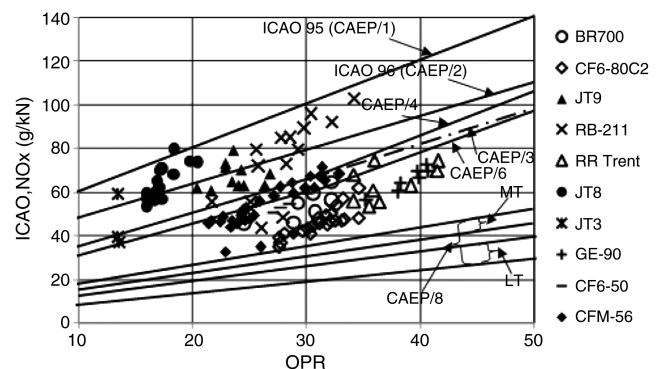Fig. 1 Evolution of NOx emission standards (data taken from [5,9]).

both engines and aircrafts. An 80% reduction of NOx (based on the technological level of 2000) is the goal set by ACARE 2020. Because of such measures, there will be more pressure on engine manufacturers to innovate new low-emissions technology. As the regulations are becoming more and more stringent, accurate prediction and assessment of emissions from engines during all phases of an aircraft mission have become essential.

III. Prediction Techniques for NOx Emission

Engine NOx emission is indicated by an index called NOx emission index (EINOx). To quantify EINOx, various techniques are proposed in the open literature. In the present work, many such techniques are brought together and classified into five general categories (Fig. 2) to assess them in a systematic way: 1) correlation-based models, 2) the $P_3 - T_3$ method, 3) fuel flow models, 4) simplified physics-based models, and 5) high-fidelity simulations. Each method has its own strengths and weaknesses, and these are discussed next.

A. Correlation-Based Models

Correlation methods are classified into empirical and semi-empirical models (Fig. 2). Empirical and semi-empirical models are further classified into two types, direct models and ratio models, all based on engine performance and emissions data obtained via combustor rig tests or full-scale engine tests at ground level, i.e., SLS and/or at altitude.

Correlation-based models tend to be the simplest of the five model types to apply, but the correlations may involve a large number of parameters to make the predictions fall within acceptable accuracy. These models typically employ data from emission measurements on a specific engine/combustor for various operating conditions: primary variables such as P_3, T_3, T_4, fuel-to-air ratio (FAR), water-to-air ratio (WAR), etc., are used for formulating the required correlation for the empirical subcategory, while the variables t_{res}, t_{form}, T_{fl}, T_{pz}, ΔP_3, V_c, etc. (which are combustor specific), in addition to the primary variables, are used for the semi-empirical subcategory. Therefore, semi-empirical models require complete details of the combustor. In the direct model, as the name implies, EINOx value can be calculated from the correlation that contains engine parameters like P_3, T_3, FAR, T_{fl}, T_{pz}, etc., directly, whereas, in the case of ratio models, ratios of engine conditions, i.e., P_3, T_3, FAR, T_{fl}, T_{pz}, etc., at an altitude and those at SLS (typically from an open source like the ICAO databank [6]) are used.

Some of the disadvantages of empirical and semi-empirical modeling are: 1) the number of input parameters in correlations is large, and a few of them are difficult to obtain; 2) some terms in the correlations may contain exponents that may significantly amplify any error in the input data; and 3) they cannot capture the effects of design change on engine emissions, because the model inputs will not be known accurately unless the engine is tested physically.

Most of the correlations available in the open literature are based on experimental work done on a specific type of engine/combustor. Hence, the correlations available in the open literature cannot be used
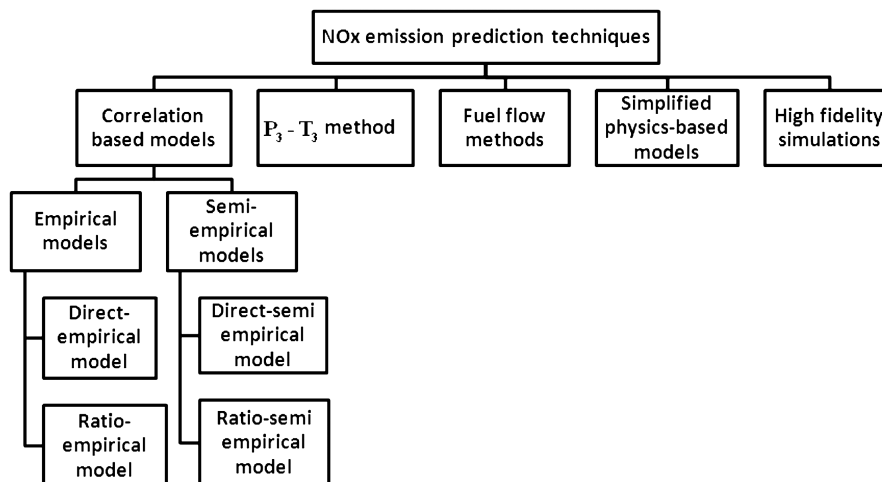

Fig. 2 Classification of prediction techniques for NOx emission.
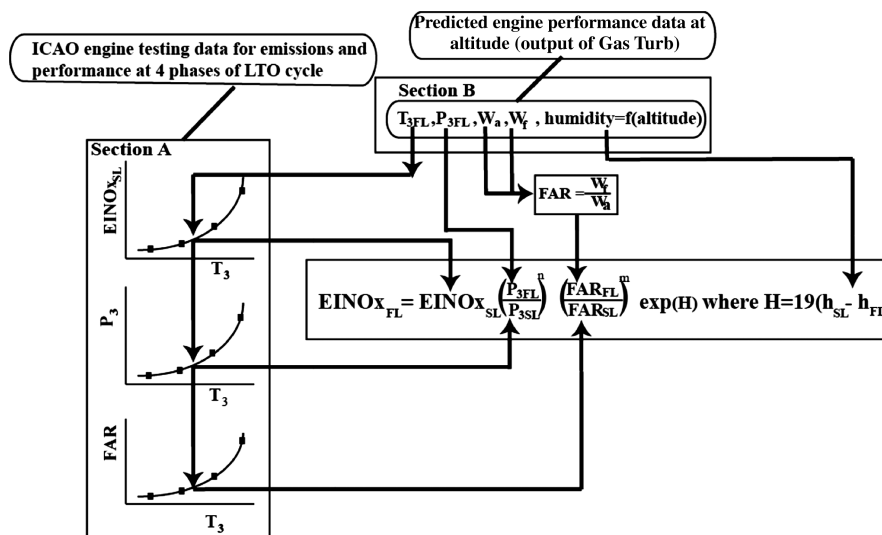

Fig. 3 Schematic of working methodology for the $P_3 - T_3$ method.

in their original form to predict emissions for other engines. But a method of adapting a particular correlation on other engines (for which emission measurement data are available) to predict EINOx was suggested in Tsalavoutas et al. [13]. It is done by using the Simplex downhill optimization algorithm. The disadvantage is that adaptation has to be done for each engine.

B. $P_3 - T_3$ Method

Of the simple prediction methods, the most dependable [4] and popular one is the $P_3 - T_3$ method. In this method, EI measured at ground level is corrected to the conditions at altitude by using both altitude and ground level combustor operating environments. Unlike the correlation methods described previously, the $P_3 - T_3$ method can be applied to all engines (i.e., using the same values of the exponent m and n). However, if greater accuracy is needed, then engine-specific values of the exponents are used.

Steps to be followed for calculating EINOx are:

1) First, combustor inlet conditions P_3, T_3, and FAR (corresponding to four throttle settings given in the ICAO databank) are determined using a gas turbine simulation software like GasTurb [14] (to be explained later). As in Fig. 3, P_3 and FAR determined previously are plotted against the combustor inlet temperature T_3 corresponding to four throttle settings. Similarly, EINOx$_{SL}$ values from the ICAO databank are also plotted against T_3 value corresponding to four throttle settings (Fig. 3).

2) Combustor inlet conditions (P_{3FL}, T_{3FL}) for the altitude in question [shown in Section B of Fig. 3] are determined, using, for example, GasTurb, for the known fuel flow from [15]. The values of EINOx$_{SL}$, P_{3SL}, FAR$_{SL}$ [shown by arrows in Section A of Fig. 3] corresponding to combustor inlet temperature at altitude T_{3FL} are obtained from the previously mentioned plots.

3) EINOx$_{FL}$ can then be calculated by using corrections for the difference in combustor inlet pressure P_3 and FAR between ground level and altitude. It is done by using suitable values of pressure exponent n, FAR exponent m, and humidity factor H in Eq. (2):

$$\text{EINO x}_{FL} = \text{EINOx}_{SL} \left(\frac{P_{3FL}}{P_{3SL}}\right)^n \left(\frac{\text{FAR}_{FL}}{\text{FAR}_{SL}}\right)^m \exp(H) \qquad (2)$$

where $H = 19(h_{SL} - h_{FL})$

The disadvantage of this method is that it needs proprietary information of an engine like P_3, T_3, FAR at reference conditions, and the engine-specific exponents. It is observed that pressure exponent n of 0.4 and FAR exponent m of zero are the best ones to use if the engine-specific exponents are not known.

C. Fuel Flow Methods

The use of the $P_3 - T_3$ method requires access to proprietary information of the engine/combustor. If the emissions are to be estimated without the proprietary information of the engine/combustor, an alternative method is necessary that uses the data of the engine, which is publicly available. Two such methods [the Boeing fuel flow method 2 (BFFM2) [16,17] and the DLR fuel flow method [18]], called *fuel flow methods*, are proposed in the open literature and are derived from the $P_3 - T_3$ method. The parameter used in these methods is the fuel flow at altitude, which is a nonproprietary indicator of the engine power setting.

BFFM2 is a method formulated by Martin et al. in 1994, available in Appendix C of Baughcum et al. [16]. The DLR fuel flow method is formulated by the DLR, German Aerospace Center [18]. In these methods, measured EINOx$_{SL}$ has to be corrected to the conditions at altitude by using both altitude and ground level combustor operating conditions similar to the $P_3 - T_3$ method. These correction factors for BFFM2 are derived by DuBois and Paynter [17] using thermodynamic relationships and energy balances, whereas for the DLR fuel flow method they are from the DLR, German Aerospace Center. Fuel flow methods consider the influence of ambient pressure, temperature, humidity, and Mach number. The aim of the methods proposed is to calculate emissions even at cruise conditions without the need for proprietary information.

For BFFM2 [16,17],

$$W_{f_{SL}} = W_{f_{FL}} \left(\frac{\theta_{amb}^{3.8}}{\delta_{amb}}\right) e^{0.2Ma^2} \qquad (3)$$

$$\text{EINO x}_{FL} = \text{EINOx}_{SL} \left(\frac{\delta_{amb}^{1.02}}{\theta_{amb}^{3.3}}\right)^{0.5} e^H \qquad (4)$$

where $\theta_{amb} = T_{amb}/288.15$, $\delta_{amb} = P_{amb}/101.325$, and $H = 19(h_{SL} - h_{FL})$.

For the DLR fuel flow method [18],

$$W_{f_{SL}} = W_{f_{FL}} \left(\frac{\theta_i^{-0.5}}{\delta_i}\right) \qquad (5)$$

$$\text{EINO x}_{FL} = \text{EINOx}_{SL} \left(\delta_i^{0.4} \cdot \theta_i^3\right) e^H \qquad (6)$$

where $\theta_i = T_{amb}(1 + 0.2Ma^2)/288.15$, $\delta_i = P_{amb}(1 + 0.2Ma^2)^{3.5}/101.325$, and $H = 19(h_{SL} - h_{FL})$.

Steps to be followed for calculating EINOx are:

1) Fuel flow data for four throttle settings from the ICAO databank [6] must be corrected for installation effects of engine air bleed for aircraft use. These are corrected fuel flows $W_{f_{SL}}$ for fuel flows W_f listed in the ICAO databank.

2) The emission indices EINOx$_{SL}$ are plotted against $W_{f_{SL}}$ on a log10–log10 scale and are curve fitted.

3) For the known fuel flow [15] $W_{f_{FL}}$ at any altitude in question, EINOx$_{SL}$ is determined from the plot corresponding to the calculated $W_{f_{SL}}$ [from Eq. (3) or Eq. (5)]. Finally, EINOx$_{FL}$ can be estimated from T_{amb}, P_{amb}, Ma (all corresponding to the altitude in question), EINOx$_{SL}$, and a humidity correction factor H. BFFM2 is available for NOx, CO, and UHC, but the DLR fuel flow method is available only for NOx. The two methods are similar, but the ratio definition and exponent values used for the correction between ground and altitude conditions are different.

D. Simplified Physics-Based Models

The complex behavior of combustion in the gas turbine is approximately captured in the simplified physics-based models. The combustion chamber is divided into many zones based on the assumptions (reduced-order physics and chemistry), and each zone is modeled as a combination of many ideal reactors. Though computationally inexpensive, simplified physics-based models are not widely used because they cannot include the complex kinetics necessary for predicting pollutant formation and emissions [19].

E. High-Fidelity Simulations

High-fidelity simulations are the most accurate among all the models if the combustor is accurately modeled using a large number of grids and the kinetic mechanisms and a few of them are discussed. These require complete details of the combustor geometry, which are combustor specific and confidential. Reynolds-averaged Navier–Stokes solution techniques require accurate boundary conditions, which can be given only if complete details of the combustor geometry are known [20]. Direct numerical simulation for combustion captures all the continuum physics of combustion but such computations for realistic geometries and flow conditions are not practical at this moment [21]. Large-eddy simulation (LES) is the technique that attempts to overcome the previously mentioned difficulty by using a model for small-scale behavior of turbulence in combustion but at the cost of accuracy. Even then, the computational time taken for the simulation is large, which makes the LES not suitable as an emission prediction tool.

Table 2 provides data from a NASA Glenn simulation of a GE90 engine and from a simulation at the University of Manchester of a Cray T3E combustor to predict temperature and velocity fields. The table shows that the time and computing power required for the LES approach is too high to use as a design or policy making tool.

Table 2 Typical time taken to predict flowfields in a combustor using LES

Component	No. of iterations	No. of processors	Computational time
GE 90 combustor [22]	31,000	256	3 h, 53 min
Cray T3E combustor [23]	88,944	64	26,432 h for two residence times
Cray T3E combustor [23]	88,944	16	52,864 h for two residence times

F. Summary

From the preceding discussions, it can be concluded that most of the correlation-based models are not suitable for predicting pollutant emissions for all engines because they are valid only for the engines in which experiments are conducted. The simplified physics-based models and high-fidelity simulations use complex methodologies to estimate pollutant emissions and they cannot be used as a prediction tool for the reasons explained previously. The $P_3 - T_3$ method is the most accurate of the simple prediction techniques but it requires proprietary information. The fuel flow methods remove the necessity of proprietary information, but the accuracy deteriorates.

IV. Engine Cycles

In the ICAO databank, the available public data that are relevant for this study are 1) fuel flow rate and EINOx values for all phases of LTO cycle and 2) ambient conditions (pressure, temperature, and WAR) at the test location, bypass ratio, OPR, and maximum rated thrust for the takeoff condition only. Inlet airflow rate at takeoff is taken from a standard webpage [15]. However, the use of the $P_3 - T_3$ method (as well as other correlation-based methods) needs the values of P_3 and T_3 of the engine cycle, but these values are not available in the public databank. In this work, therefore, thermodynamic variables at various points of the engine cycle, including P_3 and T_3, are reconstructed with the help of the commercially available gas turbine performance simulation software GasTurb [14], using the data available in [6,15]. The details of the method of reconstruction are explained in Sec. IV.A. Sections IV.B and IV.C deal with the implementation of the $P_3 - T_3$ method and the comparison of its predictions with engine-specific correlation (ESC), available for two engines, the CF6-50C2 and GE-90 family, in [24].

A. Reconstruction of Engine Cycles

Six different subsonic turbofan engine cycles are reconstructed in this study: CF6-50C2, CF6-80C2, Rolls Royce Trent 892, CFM-56-5B1, GE-90-76B, and GE-90-85B. A cycle modeled after the CF6-50C2 engine is used as an example for older in-use technology and a cycle modeled after GE90-85B engine is used to represent the recent in-use technology.

Because most of the data publicly available, as discussed, are for the takeoff condition, the reconstruction of engines is carried out at this condition in GasTurb. In other words, the design point chosen in GasTurb to reconstruct the engine is the takeoff condition.

Steps to be followed to reconstruct an engine cycle are as follows.

1. Takeoff (Design Point)

1) The input data used for reconstructing an engine in GasTurb are inlet airflow [15], bypass ratio [6], OPR [6], and relative humidity (from ambient conditions [6] and WAR [6]).

2) Mechanical efficiency, intake pressure ratio, and burner pressure ratio are assumed to be 100%. Cooling airflow rates, burner part load constant, burner efficiency, and power offtake are fixed at the default value of GasTurb because they are not known.

3) In GasTurb, outer fan pressure ratio is iterated to get the optimum jet velocity ratio $(V_{jc}/V_{jh})_{op} \approx \eta_{LPT}\eta_f$ [25]. The compressor pressure ratio is then known from the input value for the OPR. Concurrently, burner exit temperature T_4 is set to iterate to match the fuel flow rate of the engine in question published in [6], while the isentropic efficiencies (fan, compressor, and turbines) are varied over sensible ranges until the computed value of thrust (i.e., the output of GasTurb simulation) match the data publicly available in [6] as closely as possible.

4) Now the thermodynamic variables at takeoff required in this study, such as P_3 and T_3, can be obtained from the output of GasTurb.

In Table 3, reconstructed cycle data thus obtained are compared with publicly available data for the design condition. The percentage error in thrust and fuel flow are also shown in Table 3.

2. Climbout, Approach, and Idle

For these phases of LTO, the engine reconstructed previously should be run in off-design mode in GasTurb. For these phases, the airflow rates are not known, so the fuel flow rates given in the ICAO databank are used instead as the input parameter. The GasTurb simulation gives the thrust produced at each of these phases as well as the respective values of P_3 and T_3.

3. Cruise

1) The cruise condition is simulated by running the reconstructed engine in GasTurb at off-design mode.

2) Ambient conditions at cruise phase are different from that of the LTO cycle; hence, it is necessary to give Ma and altitude.

3) Thermodynamic variables at cruise condition can now be obtained from the GasTurb simulation using the fuel flow rate (calculated from SFC [15] and cruise thrust [15]) as an input.

In this section, engines analyzed were separate-stream turbofan engines, but the methodology described previously could be extended to mixed-stream engines. In the case of mixed-stream engines, the optimum fan pressure ratio can be achieved using the optimum jet velocity ratio relation explained in Guha [26]. Related issues on performance and optimization of gas turbines, with nonperfect gas effects, are given in [27–29].

B. Implementation of $P_3 - T_3$ Method

The $P_3 - T_3$ method is implemented here to study the NOx emission characteristics of a particular engine at cruise condition (which is the longest phase of a mission). By the methodology described in Sec. III.B, the parameters such as P_{3SL}, T_{3SL}, and EINOx$_{SL}$ are obtained. Then the required thermodynamic variable P_{3FL} to estimate EINOx$_{FL}$ is obtained from GasTurb (off-design) by varying the combustor inlet temperature at altitude conditions T_{3FL} instead of the fuel flow rate. EINOx$_{FL}$ values, for each combination

Table 3 Comparison of reconstructed cycle data (obtained from GasTurb) and published data [6] at SLS takeoff condition

Engine	Computed and published fuel flow, kg/s	Computed thrust, kN	Published thrust, kN	% error in thrust
CF6-50C2	2.361	229.33	230.4	−0.46
CF6-80C2	2.581	266.43	267.3	−0.33
CFM-56-5B1	1.318	133.88	133.4	0.36
Rolls Royce Trent 892	3.91	411.16	411.48	−0.08
GE-90-76B	2.824	359.92	360.62	−0.19
GE-90-85B	3.169	395.12	395.31	−0.05

of P_{3FL} and T_{3FL}, are calculated [using Eq. (2)] and plotted (Fig. 4) against respective T_{3FL} values to study the NOx emission characteristics of the engine in question.

C. Comparison of $P_3 - T_3$-Predicted NOx Emission Index and Engine-Specific Correlations

ESC is a correlation derived by employing data from emission measurements on a specific engine/combustor for various operating conditions. These correlations predict EINOx value accurately only for the engine in which measurements are carried out. From the open literature, two such ESCs (with P_3, T_3, and WAR as parameters) are available: one for CF6-50C2 [Eq. (7)], which is of a single annular combustor (SAC) type, and another for the GE90 family [Eq. (8)], which is of a double annular combustor (DAC) type. They can be used to predict EINOx for all operating conditions of an engine due to the presence of the humidity correction term, which varies with altitude.

For ESCs (Table 6 in [24]),

$$\text{EINOx}_{(CF-50-C2)} = 1.35 \cdot 0.0986 \cdot \left(\frac{P_3}{1\text{atm}}\right)^{0.4}$$

$$\cdot \exp\left(\frac{T_3}{194.4} - \frac{H}{53.2 \text{ g H}_2\text{O/kg dryair}}\right) + 1.7 \qquad (7)$$

$$\text{EINOx}_{(GE90)} = 0.0986 \cdot \left(\frac{P_3}{1\text{atm}}\right)^{0.4}$$

$$\cdot \exp\left(\frac{T_3}{194.4} - \frac{H}{53.2 \text{ g H}_2\text{O/kg dryair}}\right) \qquad (8)$$

where $H = 1000 \cdot \text{WAR}$.

P_{3FL}, T_{3FL}, and WAR at flight level (FL) obtained by the application of GasTurb are used to estimate EINOx$_{FL}$ from ESCs [Eqs. (7) and (8)]. The EINOx$_{FL}$ value can also be calculated by the $P_3 - T_3$ method (as explained in Sec. IV.B); this can then be compared with the value predicted by ESC in the following two cases: case 1 [EINOx$_{FL(P_3-T_3)}$, with the EINOx$_{SL}$ value derived from the ICAO databank [6], versus EINOx$_{FL(ESC)}$] and case 2 [EINOx$_{FL(P_3-T_3)}$, with EINOx$_{SL}$ predicted by Eq. (7) or Eq. (8) with appropriate WAR from [6], versus EINOx$_{FL(ESC)}$].

This comparison is done for both the SAC (e.g., CF6-50C2) and DAC (GE-90-85B, GE-90-76B) type of combustors, and the graphs are plotted in Fig. 4.

It is observed from Fig. 4 that, for case 1 (Figs. 4a–4c), the difference between EINOx values predicted by the $P_3 - T_3$ method and by ESC is more than that for case 2 (Figs. 4d–4f). Table 4 explains the underlying reason for this: the EINOx values predicted by the ESC [i.e., Eq. (7) or Eq. (8)] at four ICAO throttle settings do not agree well with the EINOx$_{SL}$ values given in the databank, the maximum deviation being 24.99% for SAC and 151.07% for DAC. This means that when the deviation between tested EINOx$_{SL}$ values of an engine for the ICAO certification and experimental EINOx values (used for formulating the ESC) is less, EINOx values predicted by the $P_3 - T_3$ method match well with those by the ESC (as in case 2, which can be inferred from Figs. 4d–4f). Thus, the $P_3 - T_3$ method (when the ESC is not available) is a good, simple prediction technique for EINOx emissions if sufficient engine details are available to reconstruct the engine.

V. Results and Discussion

This section covers comparison of various methods for NOx prediction with the $P_3 - T_3$ method and a proposal of a new emission prediction tool obtained by modifying an existing technique.

A. Comparison of Various Methods for NOx Prediction

A classification of various NOx prediction methods has been presented in Sec. III and Fig. 2. A list of major correlation-based NOx prediction methods is collated together in the Appendix for ready
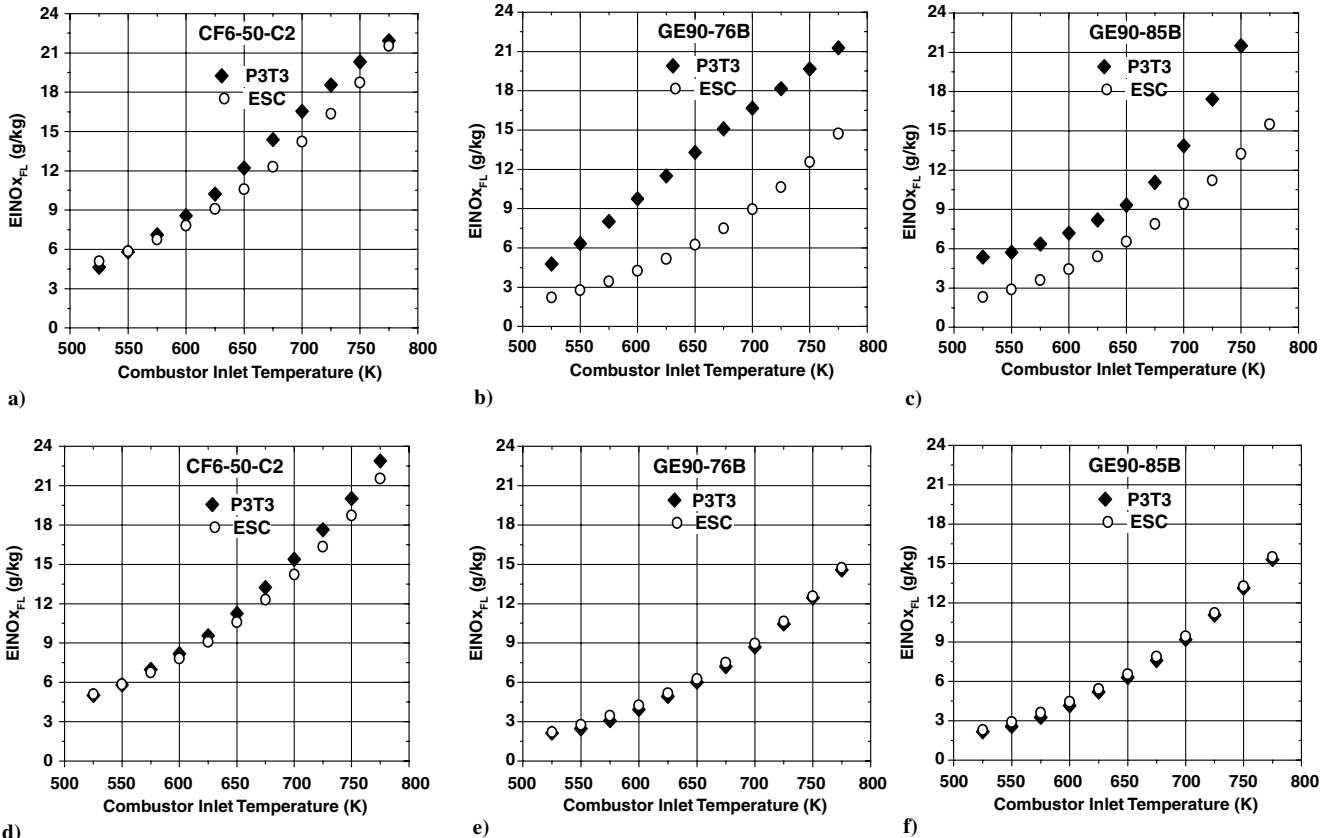

Fig. 4   Comparison of ESC with the $P_3 - T_3$ method having EINOx$_{SL}$ value a–c) derived from the ICAO databank [6] and d–f) predicted by Eq. (7) or Eq. (8) with appropriate WAR from [6].

Table 4   Comparison of EINOx values calculated from ESCs (Table 6 in [24]) for four throttle settings
with those of the ICAO engine emissions databank [6] values

Engine	Throttle settings	EINOx from ICAO databank [6]	EINOx calculated from Eq. (7) or Eq. (8) (WAR from [6])	Percentage difference
CF6-50C2	Takeoff	28.97	32.21	−10.08
CF6-50C2	Climbout	25.50	25.43	0.27
CF6-50C2	Approach	10.16	9.62	5.58
CF6-50C2	Idle	3.4	4.53	−24.99
GE-90-85B	Takeoff	52.01	30.87	68.48
GE-90-85B	Climbout	40.27	23.52	71.21
GE-90-85B	Approach	10.3	6.99	47.27
GE-90-85B	Idle	6.01	2.39	151.07
GE-90-76B	Takeoff	40.11	31.55	27.13
GE-90-76B	Climbout	31.59	24.07	31.27
GE-90-76B	Approach	15.55	7.19	116.18
GE-90-76B	Idle	5.43	2.43	123.01

reference. NOx correlations proposed by Becker et al. (as cited in [13]), Odgers and Kretchmer (Eq. 9.8 in [30]), Rizk and Mongia (Eq. 2 in [7]), and Lefebvre (Eq. 1 in [31]) belong to the direct semi-empirical model because they involve combustor parameters like t_{res}, t_{form}, T_{FL}, T_{pz}, ΔP_3, V_c, etc. The direct empirical model includes the correlations proposed by Blazowski (Eq. 11 in [32]), Lipfert (Eq. B4 in [8]), the European Association of Aerospace Industries (AECMA) (Eq. B15 in [8]), NASA (Eq. 1 in [33]), the numerical propulsion system simulation (NPSS) tool (Eq. 1.4 in [34]), the one proposed in the GasTurb User manual [14], and a modified model based on the GasTurb correlation proposed by Morales and Hall [35] because they do not contain any combustor parameters. The correlation proposed by Dopelheuer and Lecht (Eq. 3 in [18]) belongs to the ratio semi-empirical model because it has T_{pz} as a parameter, whereas the one proposed by Deidewig and Dopelheuer (Eq. 1 in [36]) is a ratio empirical model. As discussed in Sec. III.A, the semi-empirical models require complete details of the combustor, and hence they cannot be used as prediction tools as easily as empirical models (both direct and ratio types). However, empirical models also require information like P_{3FL} and T_{3FL} for a particular engine, which has been obtained in this work from gas turbine simulation software like GasTurb by following the methodology described earlier.

In Fig. 5, various methods that do not require combustor parameters like t_{res}, t_{form}, T_{FL}, T_{pz}, ΔP_3, V_c, etc., are compared for the same sets of P_{3FL} and T_{3FL} values (obtained from GasTurb). The comparative study is done in two graphs for each engine, and in total three engines are analyzed: three SAC (CFM-56-5B1, CF6-80C2, and Rolls Royce Trent 892) and a DAC (GE-90-85B). Because the $P_3 - T_3$ method is a good, simple prediction technique, all empirical models and fuel flow methods are compared with it. The left side of Fig. 5 compares six different NOx prediction methods with the $P_3 - T_3$ method, and the right side compares five more NOx prediction methods with the $P_3 - T_3$ method. Because the EINOx data points predicted by various methods for all engines in Fig. 5 are fairly close to each other, numerical values of all these points are provided here in Table 5 for easy comparison.

The following observations can be made from Fig. 5:

1) EINOx values predicted by fuel flow methods, which do not require proprietary information, lie within ±10% of that of the value predicted by the $P_3 - T_3$ method for SAC, and the deviation of above ±10% at few points is observed when used for DAC. This is so because fuel flow methods are not conceived for DAC combustors in which the main dome and the pilot domes are not working in the same way [4].

2) Though the correlation proposed by Deidewig and Dopelheuer (Eq. 1 in [36]) takes the ICAO databank value [6] as a reference, it does not predict well for all engines. A main contributory factor is that the correlation takes only the takeoff value as the reference and it does not capture the trend of EINOx variation of an engine over other phases of the LTO cycle.

3) Correlations of Blazowski, AECMA, and NASA predict well for SAC type combustor but not for the DAC type.

4) The correlation proposed by Lipfert (Eq. B4 in [8]) overpredict for all the engines analyzed in this paper.

5) GasTurb correlation and the method suggested by Morales and Hall [35] do not compare well with the $P_3 - T_3$ method for all the engines analyzed here (reasons are explained next).

6) EINOx values predicted by the new tool developed here, named *NOx: generic* in Fig. 5, compare with that of the $P_3 - T_3$ method better than other correlation-based methods and also better than the fuel flow methods in some cases (e.g., for DAC type combustors).

In GasTurb [14], EINOx is calculated from S_{NOx}: the NOx severity index. S_{NOx} is determined from Eq. (9):

$$S_{NOx} = \left(\frac{P_3}{2965}\right)^{0.4} \cdot \exp\left(\frac{T_3 - 826}{194} + \frac{6.29 - 100 \cdot WAR}{53.2}\right) \quad (9)$$

EINOx in GasTurb [14] is calculated from S_{NOx} by multiplying it by 32 for engines having conventional SAC combustors and by 23 for engines having DAC combustors. One can draw a graph of EINOx (obtained from [6]) versus S_{NOx} [obtained from Eq. (9)] at SL conditions. From this graph, one observes that the factors 32 and 23 used in GasTurb represent approximately the slope of a straight-line fit through the data of EINOx versus S_{NOx}.

It is, however, observed in this study that the GasTurb method is an oversimplification because the factor 32 does not apply for all SAC engines (similarly, the factor 23 does not apply for all DAC engines). This fact leads to the large deviation between the $EINOx_{FL}$ value estimated by the $P_3 - T_3$ method and by GasTurb, as seen in Fig. 5. From Fig. 5, it can be observed that the deviation between the $EINOx_{FL}$ value predicted by the $P_3 - T_3$ method and by GasTurb is small for CF6-80C2 (SAC), for which the slope of the ICAO $EINOx_{SL}$ versus S_{NOx} curve is 28.08 (which is close to 32), but the deviation in prediction is large for CFM-56-5B1 (which also uses SAC) because the aforementioned slope is 18.2 in this case (which is very different from 32).

To avoid the preceding difficulty, a method is suggested by Morales and Hall [35] in which the number representing the slope will be chosen as per the actual $EINOx_{SL}$ variation over the LTO cycle of an engine. For the engine in question, the $EINOx_{SL}$ values from the ICAO databank [6] and S_{NOx} are fitted in the form $EINOx_{SL} = C \cdot S_{NOx}$, where S_{NOx} at each throttle setting is calculated from Eq. (9) with respective P_3 and T_3 values and with WAR from [6]. Having determined the value of the constant C under SL conditions, $EINOx_{FL}$ can now be estimated using the same C from the relation $EINOx_{FL} = C \cdot S_{NOx(FL)}$, where $S_{NOx(FL)}$ is calculated from Eq. (9) with P_{3FL} and T_{3FL} values, and with WAR corresponding to the conditions at altitude.

B.   New Prediction Tool for NOx Emission (NOx: Generic)

Calculations of the present work, depicted in Fig. 5, demonstrates that the modification suggested by Morales and Hall [35] does not seem to work well for all cases; in fact in some cases (as shown in

a)

b)

c)

d)

e)

f)

g)

h)

♦ P3T3 [4]   □ BFFM2 ([16], [17])   △ DLR [18]   × GasTurb [14]

○ NOx: generic   + Morales [35]   − Deidewig [36]   ◇ Blazowski [32]

▲ AECMA [8]   � NASA [33]   ● NPSS [34]   ■ Lipfert [8]

Fig. 5   Comparison of various NOx prediction methods.

Figs. 5a, 5c, and 5e) the predictions are worse than the original GasTurb method [14]. Morales and Hall [35] make the tacit assumption that the linear fit for $EINOx_{SL}$ versus S_{NOx} [calculated by Eq. (9)] always passes through the origin. It is discovered during the present investigation that a linear fit for the $EINOx_{SL}$ values for most

of the tested engines listed in the ICAO databank [6] does not pass through the origin.

From a study on various engines it is found here that a relation of the form $EINOx_{SL} = C_1 \cdot S_{NOx\ Eq.\ (9)} + C_2$ fits the $EINOx_{SL}$ values of four ICAO throttle settings (thus capturing the actual trend of

Table 5   EINOx values of various NOx prediction methods[a]

Sl. no.	T_3, K	$P_3 - T_3$	BFFM	DLR	GasTurb	NOx: generic	Morales	Deidiwig	Blazowski	AECMA	NASA	NPSS	Lipfert
						CFM-56-5B1							
1	475	4.10	4.01	2.97	2.20	4.83	1.25	4.12	2.22	3.99	2.02	1.4	4.3
2	500	4.66	4.36	3.32	2.74	5.14	1.56	4.67	2.67	4.47	2.51	1.78	5.09
3	525	5.27	4.83	3.78	3.37	5.50	1.92	5.30	3.20	5.01	3.1	2.24	6.03
4	550	5.95	5.39	4.33	4.11	5.92	2.33	6.00	3.85	5.63	3.77	2.79	7.14
5	575	6.71	6.05	4.98	4.98	6.41	2.83	6.79	4.63	6.35	4.58	3.44	8.46
6	600	7.53	6.82	5.73	6.01	7.00	3.42	7.66	5.57	7.18	5.53	4.23	10.01
7	625	8.44	7.73	6.63	7.25	7.71	4.12	8.65	6.70	8.16	6.67	5.18	11.86
8	650	9.37	8.76	7.65	8.73	8.55	4.96	9.75	8.05	9.31	8.02	6.34	14.05
9	675	10.32	9.88	8.74	10.44	9.52	5.93	10.96	9.68	10.6	9.59	7.69	16.63
10	700	11.31	11.03	9.88	12.38	10.62	7.04	12.27	11.64	12	11.4	9.23	19.70
11	725	12.40	12.24	11.06	14.58	11.87	8.29	13.70	13.99	13.6	13.4	11	23.33
						CF6-80-C2							
1	475	3.42	3.19	2.68	2.18	3.53	1.91	5.34	2.22	3.97	2	1.38	4.3
2	500	3.92	3.71	3.19	2.71	4.00	2.38	6.10	2.67	4.44	2.49	1.76	5.09
3	525	4.65	4.42	3.89	3.37	4.58	2.96	6.98	3.20	5.02	3.1	2.25	6.03
4	550	5.53	5.29	4.75	4.15	5.27	3.64	7.97	3.85	5.68	3.82	2.83	7.14
5	575	6.54	6.33	5.77	5.06	6.06	4.44	9.07	4.63	6.44	4.65	3.51	8.46
6	600	7.65	7.53	6.95	6.13	7.01	5.38	10.30	5.57	7.31	5.64	4.33	10.01
7	625	8.86	8.96	8.36	7.43	8.14	6.52	11.68	6.70	8.35	6.83	5.34	11.86
8	650	10.19	10.53	9.90	8.94	9.47	7.85	13.20	8.05	9.54	8.22	6.53	14.05
9	675	11.68	12.18	11.53	10.69	11.00	9.38	14.85	9.68	10.9	9.83	7.92	16.63
10	700	13.33	13.86	13.18	12.66	12.73	11.11	16.63	11.64	12.3	11.6	9.49	19.70
11	725	15.16	15.54	14.84	14.84	14.65	13.02	18.55	13.99	13.8	13.6	11.2	23.33
						Rolls Royce Trent 892							
1	525	4.89	3.56	3.84	3.17	5.10	2.63	7.36	3.20	4.79	2.91	2.08	6.03
2	550	5.48	4.64	4.89	3.94	5.74	3.28	8.40	3.85	5.45	3.63	2.65	7.14
3	575	6.36	6.05	6.27	4.88	6.52	4.06	9.58	4.63	6.24	4.49	3.36	8.46
4	600	7.48	7.75	7.92	5.99	7.44	4.98	10.91	5.57	7.16	5.51	4.21	10.01
5	625	8.75	9.73	9.86	7.29	8.53	6.06	12.39	6.70	8.21	6.71	5.22	11.86
6	650	10.12	11.97	12.05	8.82	9.79	7.33	14.04	8.05	9.41	8.11	6.43	14.05
7	675	11.63	14.47	14.49	10.63	11.30	8.84	15.88	9.68	10.81	9.78	7.88	16.63
8	700	13.54	17.07	17.03	12.78	13.08	10.62	17.91	11.64	12.43	11.75	9.61	19.70
9	725	15.83	19.75	19.65	15.30	15.18	12.72	20.15	13.99	14.29	14.07	11.68	23.33
10	750	18.44	22.56	22.39	18.18	17.58	15.11	22.59	16.82	16.35	16.72	14.06	27.63
11	775	21.27	25.30	25.07	21.41	20.26	17.80	25.21	20.22	18.56	19.69	16.73	32.72
						GE90-85B							
1	525	5.36	3.56	3.84	2.24	3.97	3.41	9.00	3.20	4.74	2.87	2.04	6.03
2	550	5.73	4.64	4.89	2.82	4.84	4.28	10.28	3.85	5.42	3.6	2.63	7.14
3	575	6.35	6.05	6.27	3.50	5.89	5.33	11.75	4.63	6.23	4.48	3.35	8.46
4	600	7.19	7.75	7.92	4.31	7.12	6.56	13.39	5.57	7.17	5.52	4.22	10.01
5	625	8.20	9.73	9.86	5.26	8.55	7.99	15.23	6.70	8.23	6.72	5.24	11.86
6	650	9.34	11.97	12.05	6.36	10.23	9.67	17.26	8.05	9.43	8.13	6.45	14.05
7	675	11.07	14.47	14.49	7.66	12.20	11.64	19.50	9.68	10.8	9.8	7.9	16.63
8	700	13.86	17.07	17.03	9.16	14.49	13.93	21.92	11.64	12.4	11.7	9.58	19.70
9	725	17.42	19.75	19.65	10.89	17.11	16.55	24.55	13.99	14.1	13.9	11.5	23.33
10	750	21.50	22.56	22.39	12.85	20.10	19.54	27.42	16.82	16.1	16.4	13.8	27.63
11	775	25.76	25.30	25.07	15.04	23.43	22.87	30.50	20.22	18.1	19.2	16.3	32.72

[a]From [15], M = 0.8 for CFM56 and CF6-80C2, and M = 0.83 for GE90 and Trent. Altitude=10,668 m for all engines.

EINOx variation of the engine over all the phases of LTO cycle) better than $\text{EINOx}_{\text{SL}} = C \cdot S_{\text{NOx}}$, suggested in [35].

EINOx_{FL} can now be estimated by the relation $\text{EINOx}_{\text{FL}} = C_1 \cdot S_{\text{NOx(FL) Eq. (9)}} + C_2$, where the same constants C_1 and C_2 determined under SL conditions (described in the previous paragraph) are used. The relation thus proposed is the new prediction tool, NOx: generic, which satisfies two important aims of this study in the sense that it is a generic prediction method, as the name implies, without requiring any sensitive proprietary information (like pressure exponent n and FAR exponent m), and at the same time it compares well with the $P_3 - T_3$ method. However, this new tool requires P_3 and T_3 values for both SL and FL conditions, which can be obtained from gas turbine simulation software like GasTurb.

VI.   Conclusions

Many important computational tools for the prediction of EINOx are brought together in this paper, and a systematic study is performed by comparing them with the most dependable method (preferred by the industries), called the $P_3 - T_3$ method. It is observed that all the methods discussed in this paper either underpredict or overpredict the value of EINOx as compared with the

$P_3 - T_3$ method. A new prediction method proposed in this paper (represented as NOx: generic in Fig. 5) is simple and does not require sensitive proprietary information, and at the same time its prediction of EINOx compares well with that of the $P_3 - T_3$ method. The new prediction method has been applied in this paper for various engines from three major aeroengine manufacturers, and the same formulation works well for all cases examined.

Which of the many methods for the prediction of NOx emission discussed in the present paper would be used in practice would depend on what data and software are available. We have shown that if a gas turbine performance software like GasTurb is available then the $P_3 - T_3$ method can be used with the ICAO databank (by calculating appropriate values of P_3 and T_3 at all four phases of the LTO cycle and at cruise condition), but this method would be most accurate if engine-specific values of the exponents m and n are known. The method proposed in the present work (NOx: generic, Sec. V.B) does not require any engine-specific proprietary information (such as m and n) but still needs the application of a gas turbine performance software like GasTurb. When such softwares are not available, the fuel flow methods (Sec. III.C) may provide the best compromise.

Appendix: NOx Prediction Methods Available in the Open Literature

I. List of Correlation-Based Models

1) For Rizk and Mongia (Eq. 2 in [7]),

$$\text{EINOx} = \frac{15 \times 10^{14} \cdot t_{\text{res}}^{0.5} \cdot \exp(\frac{-71,100}{T_{\text{fl}}})}{P_3^{0.03}(\frac{\Delta P_3}{P_3})^{0.5}}$$

2) For Lipfert (Eq. B4 in [8]),

$$\text{EINOx} = 0.17282 \cdot \exp(0.00676593 T_3)$$

3) For AECMA (Eq. B15 in [8]),

$$\text{EINOx} = 2 + 28.5 \sqrt{\frac{P_3}{3100}} \exp\left(\frac{T_3 - 825}{250}\right)$$

4) For Becker et al. (as cited in [13]),

$$\text{NOx (ppmv)} = 5.73 \times 10^{-6} \cdot \exp(0.00833 T_{\text{fl}}) P_3^{0.5}$$

5) For GasTurb [14],

$$S_{\text{NOx}} = \left(\frac{P_3}{2965}\right)^{0.4} \exp\left(\frac{T_3 - 826}{194} + \frac{6.29 - 100 \cdot \text{WAR}}{53.2}\right)$$

6) For Dopelheuer and Lecht (Eq. 3 in [18]),

$$\text{EINOx} = \text{EINOx}_{\text{SL}} \left(\frac{P_{3_{\text{FL}}}}{P_{3_{\text{SL}}}}\right)^{0.5} \left(\frac{T_{3_{\text{SL}}}}{T_{3_{\text{FL}}}}\right)^{0.5} \left(\frac{T_{\text{pz}_{\text{SL}}}}{T_{\text{pz}_{\text{FL}}}}\right)^{1.5}$$

$$\times \exp\left[38,000\left(\frac{1}{T_{\text{fl}_{\text{SL}}}} - \frac{1}{T_{\text{fl}_{\text{FL}}}}\right)\right]$$

7) For Odgers and Kretchmer (Eq. 9.8 in [30]),

$$\text{EINOx} = 29 \cdot \exp\left(\frac{-21670}{T_{\text{fl}}}\right) P_3^{0.66}[1 - \exp(-250 t_{\text{form}})]$$

8) For Lefebvre (Eq. 1 in [31]),

$$\text{EINOx} = 4.59 \times 10^{-9} \cdot P_3^{0.25} \cdot F \cdot t_{\text{res}} \cdot \exp[0.01(T_{\text{fl}} + 273)]$$

9) For Blazowski (Eq. 11 in [32]),

$$\text{EINOx} = 10^{\left[1 + 0.0032(T_3 - 581.25)\sqrt{\frac{P_{\text{amb}_{\text{FL}}}}{P_{\text{amb}_{\text{SL}}}}}\right]}$$

10) For NASA (Eq. 1 in [33]),

$$\text{EINOx} = 33.2 \cdot \left(\frac{p_3}{432.7}\right)^{0.4} \cdot \exp\left(\frac{t_3 - 459.67 - 1027.6}{349.9}\right.$$

$$\left. + \frac{6.29 - 6.3}{53.2}\right)$$

11) For NPSS (Eq. 1.4 in [34]),

$$\text{EINOx} = 0.068 \cdot p_3^{0.5} \cdot \exp\left(\frac{t_3 - 459.67}{345}\right) \cdot \exp(H)$$

12) For Deidewig and Dopelheuer (Eq. 1 in [36]),

$$\text{EINOx} = \text{EINOx}_{\text{SL(TO)}} \cdot \frac{\exp(\frac{135000}{RT_{\lambda_{\text{SL}}}})}{\exp(\frac{135000}{RT_{\lambda_{\text{FL}}}})} \cdot \frac{P_{3_{\text{FL}}}}{P_{3_{\text{SL(TO)}}}} \cdot \frac{W_{a_{\text{SL(TO)}}}}{W_{a_{\text{FL}}}} \cdot \frac{T_{3_{\text{SL(TO)}}}}{T_{3_{\text{FL}}}}$$

where $T_\lambda = 2281[P_3^{0.009375} + 0.000178 P_3^{0.005}(T_3 - 298)]$.

II. $P_3 - T_3$ Method

The $P_3 - T_3$ method is described in [4]:

$$\text{EINO x}_{\text{FL}} = \text{EINOx}_{\text{SL}} \cdot \left(\frac{P_{3\text{FL}}}{P_{3\text{SL}}}\right)^n \left(\frac{\text{FAR}_{\text{FL}}}{\text{FAR}_{\text{SL}}}\right)^m \exp(H)$$

where $H = 19(h_{\text{SL}} - h_{\text{FL}})$.

III. Fuel Flow Methods

1) For BFFM2 [16,17],

$$W_{f_{\text{SL}}} = W_{f_{\text{FL}}}\left(\frac{\theta_{\text{amb}}^{3.8}}{\delta_{\text{amb}}}\right)e^{0.2\text{Ma}^2} \quad \& \quad \text{EINOx}_{\text{FL}} = \text{EINOx}_{\text{SL}}\left(\frac{\delta_{\text{amb}}^{1.02}}{\theta_{\text{amb}}^{3.3}}\right)^{0.5} e^H$$

where $\theta_{\text{amb}} = T_{\text{amb}}/288.15$, $\delta_{\text{amb}} = P_{\text{amb}}/101.325$, and $H = 19(h_{\text{SL}} - h_{\text{FL}})$.

2) For the DLR fuel flow method [18],

$$W_{f_{\text{SL}}} = W_{f_{\text{FL}}}\left(\frac{\theta_i^{-0.5}}{\delta_i}\right) \quad \& \quad \text{EINOx}_{\text{FL}} = \text{EINOx}_{\text{SL}} \cdot \left(\delta_i^{0.4} \cdot \theta_i^3\right) e^H$$

where $\theta_i = T_{\text{amb}}(1 + 0.2Ma^2)/288.15$, $\delta_i = P_{\text{amb}}(1 + 0.2Ma^2)^{3.5}/101.325$, and $H = 19(h_{\text{SL}} - h_{\text{FL}})$.

References

[1] Haglind, F., Hasselrot, A., Singh, R., "Potential of Reducing the Environmental Impact of Aviation by Using Hydrogen Part 1: Background, Prospects and Challenges," *Aeronautical Journal*, Vol. 110, No. 1110, Aug. 2006, pp. 533–540.

[2] Barrett, S. R. H., Britter, R. E., and Waitz, I. A., "Global Mortality Attributable to Aircraft Cruise Emissions," *Environmental Science and Technology*, Vol. 44, No. 19, 2010, pp. 7736–7742. doi:10.1021/es101325r

[3] The Boeing Company, Boeing current market outlook 2005, http://www.boeing.com/commerical/cmo/ [retrieved 25 June 2010].

[4] Norman, P. D., Lister, D. H., Lecht, M., Madden, P., Park, K., Penanhoat, O., Plaisance, C., and Renger, K., "Development of the Technical Basis New Emissions Parameter Covering the Whole Aircraft Operation," NEPAIR, Final TR NEPAIR/WP4/WPR/01, Sept. 2003.

[5] International Civil Aviation Organization, http://www.icao.int [retrieved 20 June 2010].

[6] International Civil Aviation Organization aircraft engine emissions databank, International Civil Aviation Organization Doc. 9646-AN/943, 1st ed., 1995.

[7] Mongia, H., and Dodds, W., "Low Emissions Propulsion Engine Combustor Technology Evolution Past, Present and Future," 24th Congress of the International Council of the Aeronautical Sciences, International Council of the Aeronautical Sciences Paper 2004-6.9.2, Yokohama, Japan, 29 Aug.–3 Sept. 2004.

[8] Green, J. E., "Greener by Design: The Technology Challenge," *Aeronautical Journal*, Vol. 106, No. 1056, Feb. 2002, pp. 57–113.

[9] Donnerhack, S., "Beiträge Der Flugtriebwerke Zur Schadstoffreduktion Im Luftverkehr, Präsentation Für Mtu Aero Engines Beim Workshop," *Flugverkehr und luftqualität: partikel: und stickoxide-missionen*, Berlin, 2005.

[10] Wit, R. C. N., Boon, B. H., van Velzen, A., Cames, M., Deuber, O., and Lee, D. S., "Giving Wings to Emission Trading, Inclusion of Aviation Under the European Emission Trading System (ETS)," Design and Impacts Rept. for the European Commission ENV.C.2/ETU/2004/0074r, Delft, The Netherlands, July 2005.

[11] Recommendation of the European Civil Aviation Conference/27-4 NOx Emission Classification Scheme, European Civil Aviation Conference, https://www.ecac-ceac.org//publications_events_news/ecac_documents/resolutions_and_recommendations [retrieved 20 July 2010].

[12] Advisory Council for Aeronautics Research in Europe, http://www.acare4europe.com [retrieved 27 Aug. 2010].

[13] Tsalavoutas, A., Kelaidis, M., Thoma, N., and Mathioudakis, K., Correlations Adaptation For Optimal Emissions Prediction, *Proceedings of GT2007: ASME Turbo Expo 2007: Power for Land, Sea and Air GT2007-27060*, Montreal, May 2007.

[14] Kurzke, J., GasTurb 11. A Program to Calculate Design and Off-Design Performance of Gas Turbines, 2007.

[15] Meier, N., Jet Engine Specification Database, http://www.jet-engine.net/civtfspec.html [retrieved 17 Sept. 2010].

[16] Baughcum, S. L., Tritz, T. G., Henderson, S. C., and Pickett, D. C., "Scheduled Civil Aircraft Emission Inventories for 1992: Database

Development and Analysis," NASA CR 4700, April 1996.

[17] DuBois, D., and Paynter, G. C., "Fuel Flow Method 2," Society of Automotive Engineers TP 2006-01-1987, 2006.

[18] Dopelheuer, A., and Lecht, M., "Influence of Engine Performance on Emission Characteristics," *Symposium on Gas Turbine Engine Combustion, Emissions and Alternative Fuels*, Proc. No. RTO MP-14, Lisbon, Portugal, 12–16 Oct. 1998.

[19] Seebold, J. G., Kee, R. J., Lutz, A. J., Pitz, W. J., Westbrook, C. K., and Senkan, S., "Emissions of Volatile Organic Compounds from Stationary Combustion Sources: Numerical Modeling Capabilities," *Conference: 1992 American Flame Research Committee Fall International Symposium*, Cambridge, MA, Proc. No. UCRL-JC-111829; CONF-9210359-1, Oct. 1992.

[20] Allaire, D. L., Waitz, I. A., Willcox, K. E., "A Comparison of Two Methods for Predicting Emissions from Aircraft Gas Turbine Combustors," *Proceedings of GT2007: ASME Turbo Expo 2007: Power for Land, Sea and Air GT2007-28346*, Montreal, May 2007.

[21] Shinjo, J., Matsuyama, S., Mizobuchi, Y., and Ogawa, S., "Numerical Simulation of Combustion Dynamics At ISTA/JAXA," *Lecture Notes in Computer Science*, Vol. 4759, 2008, pp. 414–426.
doi:10.1007/978-3-540-77704-5_39

[22] Turner, M. G., Norris, A., and Veres, J. P., High Fidelity 3D Simulation of the GE90, AIAA Paper 2003-3996, 2003.

[23] Di Mare, F., Jones, W. P., and Menzies, K. R., "Large Eddy Simulation of a Model Gas Turbine Combustor," *Combustion and Flame*, Vol. 137, No. 3, 2004, pp. 278–294.
doi:10.1016/j.combustflame.2004.01.008

[24] Lukachko, S. P., and Waitz, I. A., "Effects of Engine Aging on Aircraft NOx Emissions," American Society of Mechanical Engineers, Rept. 97-GT-386, 1997.

[25] Guha, A., "Optimisation of Aero Gas Turbine Engines," *Aeronautical Journal*, Vol. 105, No. 1049, 2001, pp. 345–358.

[26] Guha, A., "Optimum Fan Pressure Ratio for Bypass Engines with Separate or Mixed Exhaust Streams," *Journal of Propulsion and Power*, Vol. 17, No. 5, 2001, pp. 1117–1122.
doi:10.2514/2.5852

[27] Guha, A., "Performance and Optimisation of Gas Turbines with Real Gas Effects," *Journal of Power and Energy*, Vol. 215, No 4, 2001, pp. 507–512.
doi:10.1243/0957650011538631

[28] Guha, A., "An Efficient Generic Method for Calculating the Properties of Combustion Products," *Journal of Power and Energy*, Vol. 215, No. 3, 2001, pp. 375–387.
doi:10.1243/0957650011538596

[29] Guha, A., "Effects of Internal Combustion and Nonperfect Gas Properties on the Optimum Performance of Gas Turbines," *Journal of Mechanical Engineering Science*, Vol. 217, No A4, 2003, pp. 1085–1099.
doi:10.1243/095440603322407317

[30] Lefebvre, A. H., *Gas Turbine Combustion*, 2nd ed., Edwards Brothers, Ann Arbor, MI, 1998, p. 373.

[31] Rizk, N. K., and Mongia, H. C., "Semi Analytical Correlations for NOx, CO and UHC Emissions," *Journal of Engineering for Gas Turbines and Power*, Vol. 115, No. 3, 1993, pp. 612–619.
doi:10.1115/1.2906750

[32] Mulder, T. J., and Ruijgrok, G. J. J., "On the Reduction of NOx-Emission Levels by Performing Low NOx Flights," 26th Congress of the International Council of the Aeronautical Sciences Including the Eighth AIAA Aviation Technology, Integration, and Operations Conference, International Council of the Aeronautical Sciences Paper ICAS2008-4.7 ST2, Anchorage, AK, 14–19 Sept. 2008.

[33] Daggett, D. L., *Water Misting and Injection of Commercial Aircraft Engines to Reduce Airport NOx*, NASA CR-2004-212957, 2004.

[34] Allaire, D. L., "A Physics-Based Emissions Model for Aircraft Gas Turbine Combustors," M.Sc. Thesis, Massachusetts Institute of Technology, Cambridge, MA, 2006.

[35] Morales, M. V., and Hall, C. A., "Modeling Performance and Emissions from Aircraft for the Aviation Integrated Modelling Project," *Journal of Aircraft*, Vol. 47, No. 3, 2010, pp. 812–819.
doi:10.2514/1.44020

[36] Gardner, R. M., Adams, K., Cook, T., Deidewig, F., Ernedal, S., Falk, R., Fleuti, E., Herms, E., Johnson, C. E., Lecht, M., Lee, D. S., Leech, M., Lister, D., Massi, B., Metcalfe, M., Newton, P., Schmitt, A., Vandenbergh, C., and Van Drimmelen, R., "The ANCAT/EC Global Inventory of NOx Emissions from Aircraft," *Atmospheric Environment*, Vol. 31, No. 12, 1997, pp. 1751–1766.
doi:10.1016/S1352-2310(96)00328-7

L. Maurice
Associate Editor